Wear 328-329 (2015) 356–362

Contents lists available at ScienceDirect

Wear

journal homepage: www.elsevier.com/locate/wear

Effect of counterparts on the tribological properties of TiCN coatings with low carbon concentration in water lubrication

Qianzhi Wang [a,b,c], Fei Zhou [a,b,*], Song Gao [a,b], Zhifeng Zhou [d], Lawrence Kwok-Yan Li [d], Jiwang Yan [c]

[a] State Key Laboratory of Mechanics and Control of Mechanical Structures, Nanjing University of Aeronautics and Astronautics, Nanjing, 210016, China
[b] College of Mechanical and Electrical Engineering, Nanjing University of Aeronautics and Astronautics and Jiangsu Key Laboratory of Precision and Micro-Manufacturing Technology, Nanjing, 210016, China
[c] Department of Mechanical Engineering, Faculty of Science and Technology, Keio University, Yokohama, 2238522, Japan
[d] Advanced Coatings Applied Research Laboratory, Department of Mechanical and Biomedical Engineering, City University of Hong Kong, 83 Tat Chee Avenue, Kowloon, Hong Kong, China

ARTICLE INFO

Article history:
Received 4 November 2014
Received in revised form
3 March 2015
Accepted 5 March 2015
Available online 13 March 2015

Keywords:
TiN(C) coatings
Friction
Wear
Counterpart
Water lubrication

ABSTRACT

TiN and TiCN coatings have long been used for wear reduction in application like tooling, but there are other potential industrial applications in aqueous environments. Therefore, the current investigation explores the friction and wear compatibility of TiN and TiCN coatings against potential sliding partners in water. 316 L discs coated with TiN and TiCN (containing 2.46 at% C) slid against fixed balls of Al_2O_3, SiC, Si_3N_4, and SUS440C in water. In terms of mean steady-state friction coefficient, the ranking from low to high was: SiC < Si_3N_4 < Al_2O_3 < SUS440C regardless of coating type. It is proposed that due to lubrication by silica gel, the friction coefficients and wear rates of TiCN coatings against SiC and Si_3N_4 balls were lower than those against Al_2O_3 and SUS440C balls. For the TiCN/SUS440C tribopairs, tribo-oxidation occurred easily for SUS440C ball, and the oxides on the wear track caused the highest friction coefficient and the roughest wear surfaces. But wear of the TiCN/Al_2O_3 tribopairs, which had the highest wear rate of the coatings, was dominated by abrasion. In terms of the friction and wear behavior under water-lubricated test conditions, SiC was the most suitable counterpart for TiCN-coated stainless steel.

1. Introduction

Due to a satisfactory combination of TiC, TiN and a-C with high hardness, favorable toughness and low friction coefficient [1–4], TiCN coatings have been already paid more attention in modern industry field. Polcar et al. [5] pointed out that TiCN coatings exhibited lower friction coefficient than TiN coatings under different temperatures. On the other hand, at room temperature, nc-TiCN/a-SiCN coatings showed superior tribology to nc-TiN/a-SiN coatings [6], and the similar results have been reported in Refs. [7,8]. It is worth noticing that the friction conditions in all above-mentioned literatures were dry environment. In order to meet the requirements of environment protection and energy saving, TiCN coatings have been expected to be used in water environment. Currently, favorable tribology of TiCN coatings in aqueous environment such as HBSS, seawater and water-based slurry has been covered [9–11]. Regarding the tribology of TiCN coatings in water lubrication, Wang et al. [12] reported that the TiCN/SiC tribopair exhibited low friction coefficient (0.17) and low coatings wear rate (2.3×10^{-6} mm^3/Nm). Nevertheless, the mechanical and tribological properties of TiCN coatings were subject to C concentration [13–16]. Wang et al. [17] pointed out that the TiCN coatings with the C concentration of 2.46 at% exhibited excellent tribological properties as they studied the influence of C concentration on tribological property of TiCN/SiC tribopair in water lubrication. As is known, a tribopair comprised two objects. Apart from coating itself, counterpart is also a non-ignorable factor to tribology. As seen in Table 1 [12,18–22], the friction coefficients and the coatings wear rates were governed by counterparts. Thus, if the TiN(C) coatings are expected to be used in water environment, it was imperative to select the optimal counterpart to the TiCN coatings in water lubrication. However, the research work related to the effect of counterpart on the tribological properties of TiCN coatings in water has not yet been performed.

The aim of this study is to find the optimal counterpart via comparing the friction and wear properties of TiCN coatings (2.46 at% C) sliding against Al_2O_3, SiC, Si_3N_4 and SUS440C balls in water lubrication, and to indicate the wear mechanisms of different tribopairs in water.

* Corresponding author at: State Key Laboratory of Mechanics and Control #of Mechanical Structures, Nanjing University of Aeronautics and Astronautics, Nanjing, 210016, China. Tel./fax: +86 25 84893083.
E-mail address: fzhou@nuaa.edu.cn (F. Zhou).

http://dx.doi.org/10.1016/j.wear.2015.03.007
0043-1648/

Table 1
Tribological properties of different tribopairs in previous literatures.

References	Coatings	Counterparts	Normal load	Velocity	Model	Environment	Friction coefficient	Wear
Yamane [18]	PTFE	Mild steel Bronze Alumium	10 MPa	0.036 m/s	Pin-on-disk	Dry	0.15 0.15–0.20 0.17–0.5	<120 mg <100 mg <250 mg
Wang [12]	TiCN	SiC SUJ2 SUS440C	3 N	0.100 m/s	Ball-on-disk	Deionized water	0.20 0.30 1.00	3.4×10^{-6} mm^3/Nm 1.0×10^{-6} mm^3/Nm 1.4×10^{-6} mm^3/Nm
Badiskh [19]	TiN	Al_2O_3 Ball-bear steel Mild steel Austenitic steel	2 N	0.100 m/s	Ball-on-disk	Dry 35% humidity	0.17 (25 m running-in) 0.17 (70 m running-in) 0.17 (300 m running-in) 0.90	1.3×10^{-7} mm^3/Nm 2.8×10^{-7} mm^3/Nm 2.1×10^{-7} mm^3/Nm 1.1×10^{-6} mm^3/Nm
Zhou [20]	BCN	Al_2O_3 Si_3N_4 SiC SUS440C	0.2 N	0.200 m/s	Ball-on-disk	Nitrogen	0.60 0.62 0.73 0.89	3.3×10^{-5} mm^3/Nm 5.1×10^{-5} mm^3/Nm 2.2×10^{-5} mm^3/Nm 1.1×10^{-5} mm^3/Nm
Kovalcikova [21]	SiC-HP	ZrO_2 WC–Co Al_2O_3 Si_3N_4	5 N	0.100 m/s	Ball-on-disk	Dry 30% humidity	0.45 0.46 0.50 0.62	1.6×10^{-6} mm^3/Nm 2.2×10^{-6} mm^3/Nm 3.1×10^{-6} mm^3/Nm 2.8×10^{-5} mm^3/Nm
Zhou [22]	a-CN_x	Si_3N_4 SiC SUJ2 SUS440C Al_2O_3	5 N	0.160 m/s	Ball-on-disk	Deionized water	0.013 0.017 0.072 0.075 0.100	1.5×10^{-8} mm^3/Nm 4.7×10^{-8} mm^3/Nm 2.3×10^{-8} mm^3/Nm 4.1×10^{-8} mm^3/Nm 1.8×10^{-7} mm^3/Nm

2. Experimental details

2.1. Deposition of TiN and TiCN coatings

After 316 L disks ($Ø30\times4$ mm^2) were polished by precision polishing machine (UNIPOL 802) and cleaned ultrasonically in ethanol for 10 min., the steel disk and Si(100) wafer were attached on rotating holder in the chamber of the closed-field unbalanced magnetron sputtering system (UDP-650, Teer Coatings Limited, UK). At first, the substrates were sputter cleaned by Ar^+ ion plasma at the bias voltage of -450 V, and then coated with a pure titanium interlayer ($\sim$0.2 μm) in advance. Subsequently, TiN and TiCN coatings were deposited via adjusting the sputtering current of pure titanium (Ti) and graphite (C). The specific deposition parameters are listed in Table 2.

2.2. Characterization of TiN and TiCN coatings

The coatings on Si(100) wafers were used for the characterization of microstructure and mechanical property while the coatings on 316 L discs were used for tribotests. To be specific, Raman spectroscopy (Invia RENSHAW 2000) and X-ray photoelectron spectroscopy (XPS, VG ESCALAB 220i-XL) were adopted to confirm their microstructure and element concentration. Micro-XAM™ white-light profilometer (ADE Phase-Shift, USA), Nano-Indenter XP (Nano Instruments; Inc., Oak Ridge, Tennessee) and Field Emission Scanning Electron Microscope (FE-SEM) (JEOL-JSM-7001F) were used to measure surface roughness, hardness and thickness as well as surface microstructure. The penetration depth of indentation for TiN and TiCN coatings was set as 160 nm and indentation for each sample was repeated 10 times.

2.3. Friction tests of TiN and TiCN coatings

First, according to our previous experience, the Si-based non-oxide ceramics are tribo-hydrated easily in comparison to Al_2O_3 in water, which makes them be suitable in water lubrication. Second, stainless steel is common material in current mechanical industry. Thus, Al_2O_3, SiC, Si_3N_4 and SUS440C balls (Ø8 mm) in Table 3 were chosen as counterparts. The balls roughness was measured by Surfcom-1500DX profilometer and their mechanical properties were obtained from the balls company directly. The tribological properties of coatings sliding against the four kinds of balls in deionized water were investigated using ball-on-disk tribometer (Fig. 1a). By being observed from direction *A*, the section in frame with dash line could be drawn as Fig. 1b. Prior to friction test, the radius (R) of wear track could be controlled by moving stage B in horizontal direction. The normal force (2 N) was applied on ball according to lever principle, the rotating speed (0.1 m/s) was controlled by an electric motor, and the total sliding distance was 500 m. Then a round wear track would be formed on the coatings surface. Each test was done for twice or three times to ensure the reliability of data.

Table 2
Deposition parameters of coatings.

Name	Parameter	Thickness
Atmosphere	N_2:Ar (3:10)	–
Chamber pressure	0.227 Pa	–
Temperature	Room temperature	–
Bias voltage	-60 V	–
Rotating speed of holder	10 rpm	–
Current of titanium target	8 A	–
Current of graphite target	0 A (TiN)	1.14 μm
	3 A (TiCN)	1.24 μm

Table 3
Mechanical properties of Al_2O_3, SiC, Si_3N_4 and SUS440C balls.

Counterpart balls	[a]Hardness H (GPa)	[a]Elastic modulus E (GPa)	Roughness Ra (nm)	[a]Poisson ratio ν
Al_2O_3	16.5	370	52.8	0.24
SiC	22	430	88.5	0.14
Si_3N_4	15.3	308	55.2	0.27
SUS440C	7.2	204	53.3	0.28

[a] The data were from the balls company.

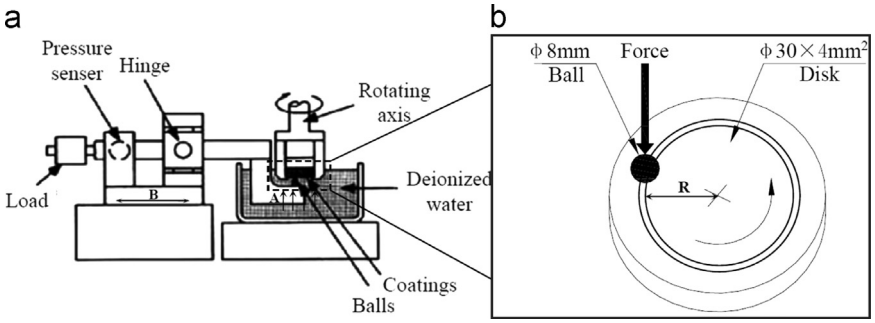

Fig. 1. Schematic diagram of (a) ball-on-disk tribometer and (b) contact between ball and disk.

After measuring the diameter (d) of wear scar on ball and the cross-section area (A) of wear track on coatings by optical microscope (XJZ-6) and Micro-XAM™ white-light profilometer, the wear rates of balls and coatings could be calculated, and this method can be found in elsewhere [12]. At last, the wear tracks of coatings were analyzed using Energy Dispersive Spectrometer (EDS) (Inca Energy 350, Oxford, UK).

3. Results and discussion

3.1. Composition and microstructure of TiN and TiCN coatings

As seen in Fig. 2, the Raman spectrum of TiN coating could be fitted into three peaks at 218, 311 and 556 cm^{-1} with Gaussian curve. According to Ref. [23], all of these peaks were definitely related to TiN. After carbon was doped in TiN coatings, besides above-mentioned TiN peaks, D peak at 1350 cm^{-1}, G peak at 1537 cm^{-1} and TiC peak at 674 cm^{-1} all appeared simultaneously in the Raman spectrum of TiCN coating. It is demonstrated that a-C phase was formed in TiCN coatings after carbon incorporation.

Fig. 3 illustrates the deconvoluted N1s spectra of TiN and TiCN coatings, which were fitted with XPS4.1 software. Three peaks including N–Ti–O bond at 396.16 ± 0.02 eV, N–Ti bond at 397.16 ± 0.02 eV and N–N bond at 398.76 eV were observed in N1s spectrum of TiN coating [24]. In contrast, the N1s spectrum of TiCN coating exhibited four peaks which originated from N–Ti–O at 396.12 eV, N–Ti–C bond at 397.07 eV, N–C bond at 398.06 eV and N=C bond at 399.19 eV [25]. In addition, the C–C bond of TiCN coatings in Ref. [17] also proved the presence of a-C phase. Thus, taking Raman and XPS results into consideration, TiCN coating consisted of TiN, TiC, a-C and a-CN_x simultaneously after carbon element was doped in the TiN coatings.

3.2. Mechanical properties of TiN and TiCN coatings

As seen in Table 4, as compared with pure TiN coating, the hardness and the reduced Young's modulus of TiCN coating increased from 20 GPa to 29 GPa and from 225 GPa to 425 GPa, respectively, but the roughness declined from 15.9 nm to 11.1 nm. According to above-mentioned results of Raman and XPS, it is clear that the increment of hardness for TiCN coatings was caused by the formation of TiC phase, which is agreement with the results in Refs. [1,3,15].

3.3. Tribological behavior of TiN and TiCN coatings sliding against four kinds of balls in water

The variation of friction coefficient of different tribopairs as a function of sliding distance in deionized water is illustrated in Fig. 4, and $\mu_{Al_2O_3}$ μ_{SiC} $\mu_{Si_3N_4}$ $\mu_{SUS440C}$ were used to symbolize the corresponding friction coefficients, respectively. No matter what

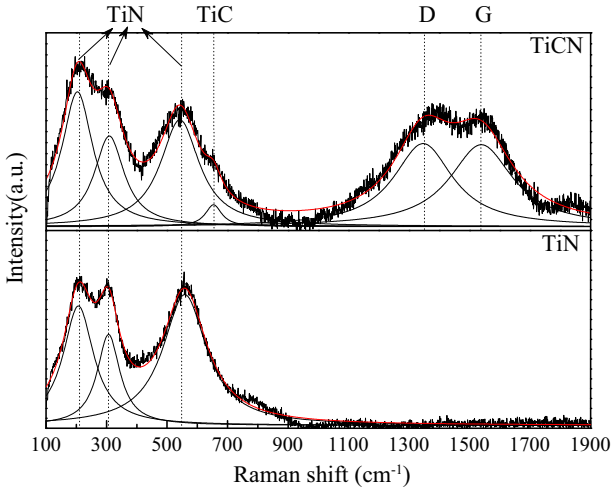

Fig. 2. Raman spectra of TiN and TiCN coatings.

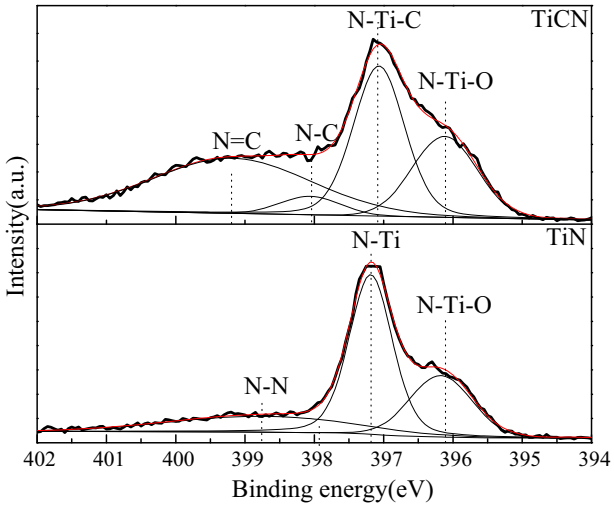

Fig. 3. Deconvoluted N1s XPS spectra of TiN and TiCN coatings.

Table 4
Mechanical properties and carbon concentration of coatings.

Coatings	*H* (GPa)	Standard deviation of *H* (GPa)	Reduced *E* (GPa)	Standard deviation of *E* (GPa)	*Ra* (nm)	Ti (at%)	C (at%)	N (at%)
TiN	20	1.2	225	12.4	15.9	46.42	0	53.58
TiCN	29	3.1	425	35.1	11.1	50.36	2.46	47.18

coatings were, the variation of μ_{SiC} and $\mu_{Si_3N_4}$ was more stable than that of $\mu_{Al_2O_3}$ and $\mu_{SUS440C}$ during total sliding period. As seen from Eqs. (1) and (2), it is obvious that the tribo-hydration reaction of SiC and Si_3N_4 balls occurred easily in water [20,22,26]

$$SiC + 2H_2O = SiO_2 + CH_4$$
$$\Delta G_f^{298} = -372.902\ \text{kJ mol}^{-1} \quad (1)$$

$$Si_3N_4 + 6H_2O = 3SiO_2 + 4NH_3$$
$$\Delta G_f^{298} = -570.346\ \text{kJ mol}^{-1} \quad (2)$$

$$Al_2O_3 + 3H_2O = 2Al(OH)_3$$
$$\Delta G_f^{298} = -25.9\ \text{kJ mol}^{-1} \quad (3)$$

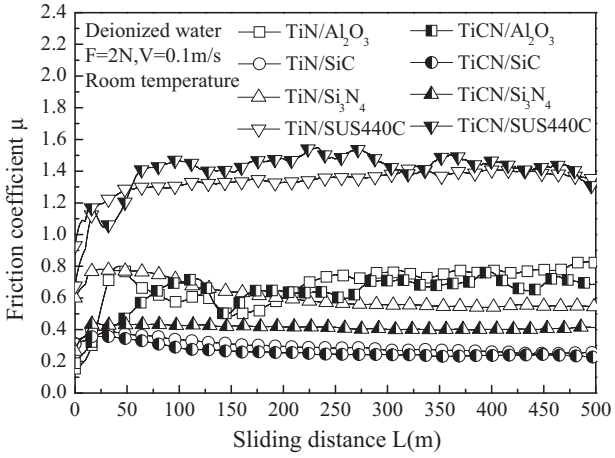

Fig. 4. Friction behaviors of TiN and TiCN coatings sliding against different balls in water at 2 N and 0.1 m/s.

Then, the generation of SiO_2 would dissolve into water to form silica gel as lubrication film which stabilized the friction coefficient. But for the coatings/Al_2O_3 tribopair, the hydration reaction hardly occurred according to Eq. (3) [27], abrasive wear dominated whole sliding process, and then the unstable friction behavior was finally obtained. Although the tribo-oxidation of SUS440C ball could occur during sliding in water, the effect of oxides was totally adverse [18]. In other word, the tribo-oxides would transfer and adhere to the wear track surface of coatings. In this case the surface roughness of friction area increased sharply, so the friction coefficient of coatings/SUS440C tribopair varied with certain amplitude. As seen in Fig. 5a, the rank of mean-steady friction coefficients $(\mu_{mAl_2O_3}, \mu_{mSiC}, \mu_{mSi_3N_4}, \mu_{mSUS440C})$

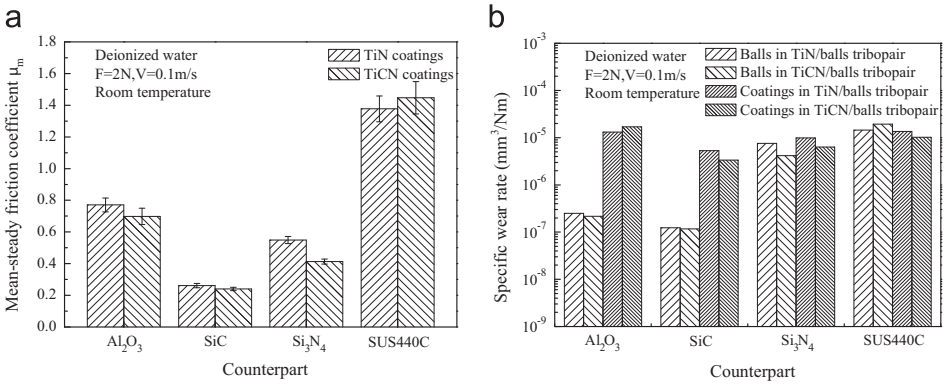

Fig. 5. Variation of (a) mean-steady friction coefficient and (b) specific wear rates of tribomaterials for different coatings/balls tribopairs in water at 2 N and 0.1 m/s.

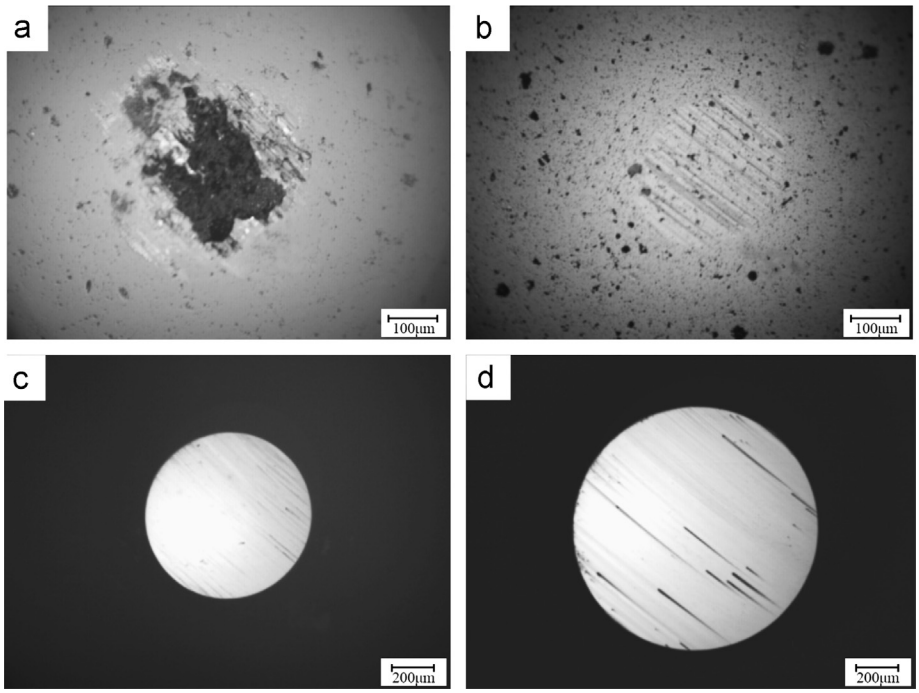

Fig. 6. Optical images of wear scars on (a)Al_2O_3 (b)SiC (c)Si_3N_4 and (d)SUS440C balls sliding against TiCN coatings.

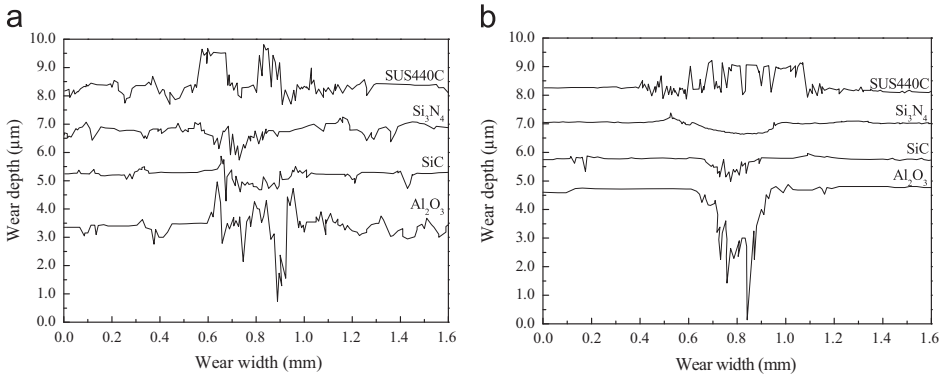

Fig. 7. Cross-sectional profiles of wear tracks on (a) TiN and (b) TiCN coatings sliding against different balls in water at 2 N and 0.1 m/s.

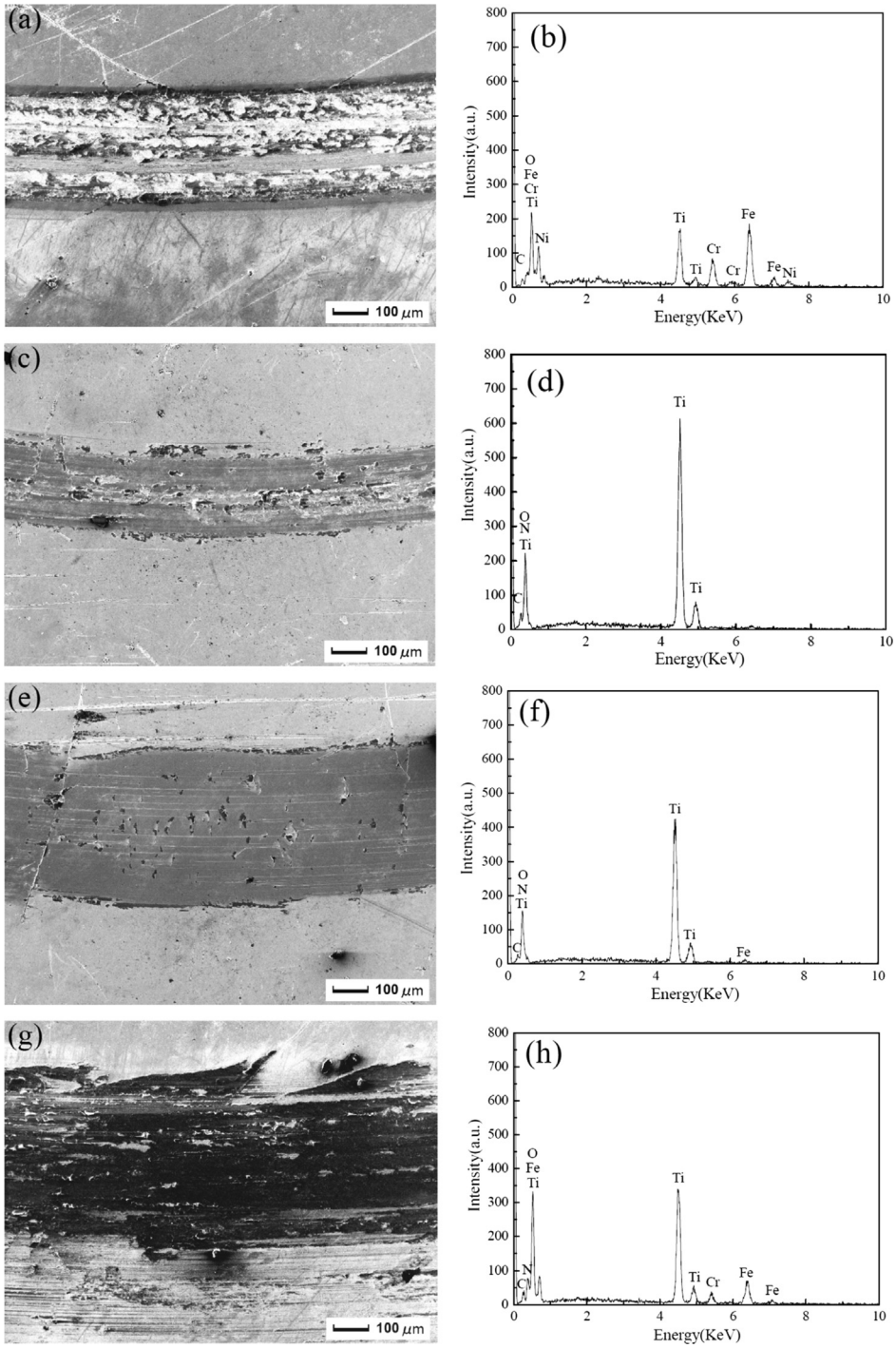

Fig. 8. FESEM images and EDS of wear tracks on TiCN coatings sliding against (a),(b) Al_2O_3 (c),(d) SiC (e),(f) Si_3N_4 and (g),(h) SUS440C balls in water at 2 N and 0.1 m/s.

were μ_{mSiC}(0.262 for TiN, 0.240 for TiCN) $<\mu_{mSi_3N_4}$(0.549, 0.413) $<\mu_{mAl_2O_3}$(0.771, 0.698) $<\mu_{mSUS440C}$(1.378, 1.447) whatever coatings were.

As seen in Fig. 5b, the specific wear rates of coatings sliding against SiC and Si_3N_4 balls (3.35–9.90 $\times 10^{-6}$ mm^3/Nm) were lower than those against Al_2O_3 and SUS440C balls (1.02–1.70 $\times 10^{-5}$ mm^3/Nm) by one order of magnitude, while the specific wear rates of Si_3N_4 and SUS440C balls were higher than those of SiC and Al_2O_3 balls. The specific wear rates of tribomaterials in the TiCN coating/SiC ball tribopair were lowest among four kinds of tribopairs. This indicated that the silica gel generated from SiC and Si_3N_4 balls could protect coatings from severe wear. For the coatings/SUS440C ball tribopair, the transfer of tribo-oxides could cause unstable friction behavior and high friction coefficient [28,29], but possess protective effect to coatings. In this case, the specific wear rates of coatings against SUS440C were even lower than those against Al_2O_3 ball. As seen in Fig. 6, for the ceramic balls, the diameter of wear scar on Si_3N_4 ball was much higher than those on SiC and Al_2O_3 balls. Actually, according to Eqs. (1)–(3), it was clear that Si_3N_4 ball was more prone to tribochemical reaction and softer than SiC and Al_2O_3 balls, which led to the highest specific wear rate of Si_3N_4 balls among three kinds of ceramic balls. But for SUS440C ball, its wear scar diameter was largest owing to tribo-oxidation and rough friction, and then its specific wear rate was further highest.

Fig. 7 shows the cross-sectional profiles of wear tracks for TiN and TiCN coatings sliding against four kinds of balls in water, while Fig. 8 displays SEM images of wear tracks on TiCN coatings with corresponding EDS analyses. It is obvious that the wear tracks profiles and surface microstructures of coatings were closely dependent on mating balls. When the TiN-based coatings slid against SUS440C balls, the depth of wear track on coatings was lower than the surface roughness (Fig. 7), the wear track surface became rough (Fig. 8g) and there were Fe, O, Cr, Ti, C and N elements detected in the wear track (Fig. 8h). This indicated that the wear oxide debris was transferred from ball to coating and adhered to friction surface. If the counterpart was Al_2O_3 ball, the wear depth and width of wear track for coatings became deeper and larger (Fig. 7), and the wear track was covered with more white wear debris (Fig. 8a). The EDS analysis showed that the Fe, Ni, Cr and O elements besides Ti, C and N elements were detected in the wear track (Fig. 8b). This showed that the coatings were worn out and wear debris was transferred from coatings to balls. When the mating balls were SiC and Si_3N_4 balls, the wear tracks became smooth and flat (Fig. 8c and e), and their wear depth became shallower and narrower, only Ti, C, N, and O elements (Fig. 8d and f) were detected. This pointed out that the tribo-chemical wear was dominated. Furthermore, it was worth noting that the wear tracks of TiCN coatings against SiC, Si_3N_4 and SUS440C balls were shallower than those of TiN coatings. This was attributed to the lubrication effect of a-C in TiCN coating. But for Al_2O_3 ball, as seen in Fig. 6a, the wear debris was transferred from coatings to Al_2O_3 ball, and then the coatings/Al_2O_3 tribopairs were gradually changed to coating/coating tribopairs during sliding friction. Although the hardness of TiCN was higher than that of TiN transfer, the contact pressure of TiCN/Al_2O_3 tribopairs was higher than that of TiN/Al_2O_3 tribopairs (Fig. 9) according to Hertzian circular point contact. Moreover, the sp^2 clusters of a-C in the TiCN coatings were largely saturated by water, which caused the a-C coatings being softened [30]. This indicated that the soft materials were easily formed on the TiCN coatings as sliding in water, and then the higher wear rate of the TiCN coatings would be obtained as sliding against Al_2O_3 balls in water (Fig. 5b).

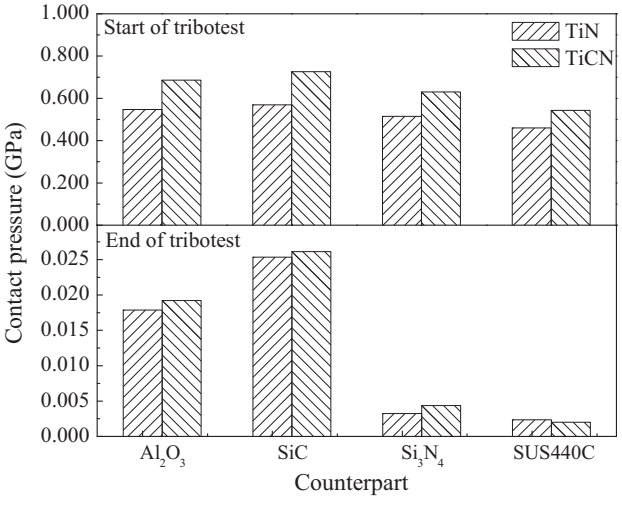

Fig. 9. Contact pressures of different tribopairs in water.

As seen in Fig. 10, the wear track microstructure of TiCN coatings against SiC balls exhibited a little difference from that against Si_3N_4 balls. Although they displayed some fatigue wear debris left, the area of fatigue wear debris on TiCN against SiC balls was larger than that against Si_3N_4 balls. This is owing to the higher contact pressure of coatings/SiC tribopair than that of coatings/Si_3N_4 tribopair (Fig. 9).

4. Conclusions

The TiN and TiCN coatings with low C concentration (2.46 at%) were deposited by using unbalanced magnetron sputtering, and their tribological properties sliding against Al_2O_3, SiC, Si_3N_4 and SUS440C balls were compared systematically, the conclusions were summarized as:

(1) TiCN coatings (2.46 at%) consisted of TiC, TiN, a-C and a-CN_x and their hardness was 29 GPa after the carbon element was doped in TiN coatings.

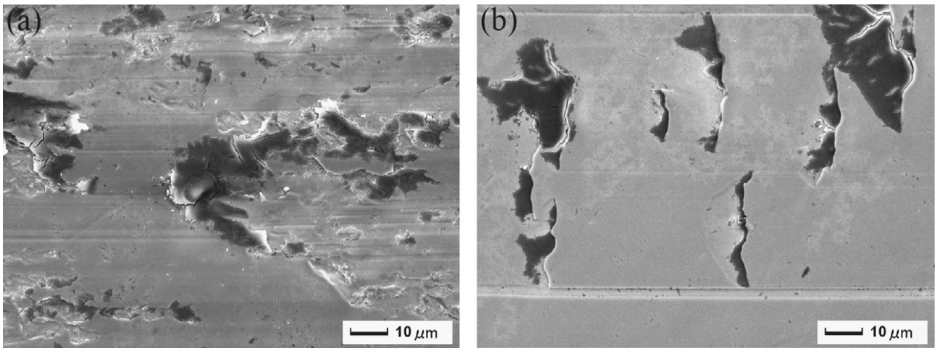

Fig. 10. Fatigue wear debris of TiCN coatings sliding against (a) SiC and (b) Si_3N_4 balls.

(2) Regardless of coatings, the rank of mean-steady friction coefficients was $\mu_{mSiC} < \mu_{mSi_3N_4} < \mu_{mAl_2O_3} < \mu_{mSUS440C}$, which was dominated by the tribochemical reactions, transfer of tribo-debris and contact pressures of tribopairs in water.
(3) The TiCN coatings sliding against SiC and Si_3N_4 balls exhibited lower specific wear rates by one order of magnitude than those against Al_2O_3 and SUS440C balls, while the specific wear rates of Si_3N_4 and SUS440C balls were much higher than those of SiC and Al_2O_3 balls.
(4) Although the higher contact pressure of coating/SiC tribopair contributed to the more fatigue wear debris in comparison to the coating/Si_3N_4 tribopair, SiC balls were the optimal counterpart to TiCN coating in water after the friction coefficient and wear rate were taken into account synthetically.

Acknowledgments

This work has been supported by National Natural Science Foundation of China (Grant no. 51375231), The Research Fund for the Doctoral Program of Higher Education (Grant no.20133218110030) and a project funded by the Priority Academic Program Development of Jiangsu Higher Education Institutions (PAPD). We would like to acknowledge them for their financial support.

References

[1] Y.H. Cheng, T. Browne, B. Heckerman, Influence of the C content on the mechanical and tribological properties of the TiCN coatings deposited by LAFAD technique, Surf. Coat. Technol. 205 (2011) 4024–4029.
[2] T. Polcar, R. Novak, P. Siroky, The tribological characteristics of TiCN coating at elevated temperatures, Wear 260 (2006) 40–49.
[3] H.C. Barshilia, M.S. Prakash, D.V.S. Rao, K.S. Rajam, Superhard nanocomposite coatings of TiN/a-C prepared by reactive DC magnetron sputtering, Surf. Coat. Technol. 195 (2005) 147–153.
[4] L. Escobar-Alarcon, V. Medina, E. Camps, S. Romero, M. Fernandez, D. Solis-Casados, Microstructural characterization of Ti–C–N thin films prepared by reactive crossed beam pulsed laser deposition, Appl. Surf. Sci. 257 (2011) 9033–9037.
[5] T. Polcar, T. Kubart, R. Novak, L. Kopecky, P. Siroky, Comparison of tribological behaviour of TiN, TiCN and CrN at elevated temperatures, Surf. Coat. Technol. 193 (2005) 192–199.
[6] S. Guruvenket, D. Li, J.E. Klemberg-Sapieha, L. Martinu, J. Szpunar, Mechanical and tribological properties of duplex treated TiN, nc-TiN/a-SiN_x and nc-TiCN/a-SiCN coatings deposited on 410 low alloy stainless steel, Surf. Coat. Technol. 203 (2009) 2905–2911.
[7] G.J. Zhang, B. Li, B.L. Jiang, F.X. Yan, D.C. Chen, Microstructure and tribological properties of TiN, TiC and Ti(C,N) thin films prepared by closed-field unbalanced magnetron sputtering ion plating, Appl. Surf. Sci. 255 (2009) 8788–8793.
[8] R. Chen, J.P. Tu, D.G. Liu, Y.J. Mai, C.D. Gu, Microstructure, mechanical and tribological properties of TiCN nanocomposite films deposited by DC magnetron sputtering, Surf. Coat. Technol. 205 (2011) 5228–5234.
[9] L. Shan, Y.X. Wang, J.L. Li, H Li, X.D. Wu, J.M. Chen, Tribological behaviours of PVD TiN and TiCN coatings in artificial seawater, Surf. Coat. Technol. 226 (2013) 40–50.
[10] X.Y. Ren, Z.J. Peng, Y.B. Hu, C.B. Wang, Z.Q. Fu, W. Yue, L.H. Qi, H.Z. Miao, Abrasive wear behavior of TiCN cermets under water-based slurries with different abrasives, Tribol. Int. 66 (2013) 35–43.
[11] A.P. Serro, C. Completo, R. Colaço, F. dos Santos, C. Lobato da Silva, J.M.S. Cabral, H. Araújo, E. Pires, B. Saramago, A comparative study of titanium nitrides, TiN, TiNbN and TiCN, as coatings for biomedical applications, Surf. Coat. Technol. 203 (2009) 3701–3707.
[12] Q.Z. Wang, F. Zhou, K. Chen, M. Wang, T. Qian, Friction and wear properties of TiCN coatings sliding against SiC and steel balls in air and water, Thin Solid Films 519 (2011) 4830–4841.
[13] Y.H. Cheng, T. Browne, B. Heckerman, TiCN coatings deposited by large area filtered arc deposition technique, J. Vac. Sci. Technol. A 28 (2010) 431–437.
[14] Y.H. Cheng, T. Browne, B. Heckerman, Influence of CH_4 fraction on the composition, structure, and internal stress of the TiCN coatings deposited by LAFAD technique, Vacuum 85 (2010) 89–94.
[15] S.W. Huang, M.W. Ng, M. Samandi, Tribological behaviour and microstructure of $TiC_xN_{(1-x)}$ coatings deposited by filtered arc, Wear 252 (2002) 566–579.
[16] L. Karlsson, L. Hultman, M.P. Johansson, J.-E. Sundgren, H. Ljungcrantz, Growth, microstructure, and mechanical properties of arc evaporated $TiC_xN_{1-x}(0 \le x \le 1)$ films, Surf. Coat. Technol. 126 (2000) 1–14.
[17] Q.Z. Wang, F. Zhou, Z.F. Zhou, Y. Yang, C. Yan, C.D. Wang, W.J. Zhang, L. K-Y. Li, I. Bello, S-T. Lee, Influence of carbon content on the microstructure and tribological properties of TiN(C) coatings in water lubrication, Surf. Coat. Technol. 206 (2012) 3777–3787.
[18] M. Yamane, T.A. Stolarski, S. Tobe, Influence of counter material on friction and wear performance of PTFE-metal binary coatings, Tribol. Int. 41 (2008) 269–281.
[19] E. Badiskh, G.A. Fontalvo, C. Mitterer, The response of PACVD TiN coatings to tribological tests with different counterparts, Wear 256 (2004) 95–99.
[20] F. Zhou, K. Adachi, K. Kato, Friction and wear behavior of BCN coatings sliding against ceramic and steel balls in various environments, Wear 261 (2006) 301–310.
[21] A. Kovalčíková, P. Kurek, J. Balko, J. Dusza, P. Šajgalík, M. Mihaliková, Effect of the counterpart material on wear characteristics of silicon carbide ceramics, Int. J. Refract. Met. Hard Mater. 44 (2014) 12–18.
[22] F. Zhou, K. Adachi, K. Kato, Friction and wear property of a-CN_x coatings sliding against ceramic and steel balls in water, Diam. Relat. Mater. 14 (2005) 1711–1720.
[23] I. Dreiling, A. Haug, H. Holzschuh, Raman spectroscopy as a tool to study cubic Ti–C–N CVD coatings, Surf. Coat. Technol. 204 (2009) 1008–1012.
[24] H. Liu, Y.H. Jiang, Z.L. Zhan, B.Y. Tang, XPS characterization of TiN layer on bearing steel surface treated by plasma immersion ion implantation and deposition technique, Spectrosc. Spect. Anal. 29 (2009) 2585–2589, in Chinese.
[25] L.C. Agudelo, R. Ospina, H.A. Castillo, A. Devia, Synthesis of Ti/TiN/TiCN coatings grown in graded form by sputtering dc, Phys. Scr. T131 (2008) 014006.
[26] Q.Z. Wang, F. Zhou, X.D. Ding, Z.F. Zhou, W.J. Zhang, L. K-Y. Li, S-T. Lee, Influences of ceramic mating balls on the tribological properties of Cr/a-C coatings with low chromium content in water lubrication, Wear 303 (2013) 354–360.
[27] D.A. Rania, Y. Yoshizawa, H. Hyuga, K. Hirao, Y. Yamauchi, Tribological behavior of ceramic materials (Si_3N_4, SiC and Al_2O_3) in aqueous medium, J. Eur. Ceram. Soc. 24 (2004) 3279–3284.
[28] X.C. Li, J.J. Lu, S.R. Yang, Effect of counterpart on the tribological behavior and tribo-induced phase transformation of Si, Tribol. Int. 42 (2009) 628–633.
[29] Z.X. Zeng, L.P. Wang, L. Chen, J.Y. Zhang, The correlation between the hardness and tribological behaviour of electroplated chromium coatings sliding against ceramic and steel counterparts, Surf. Coat. Technol. 201 (2006) 2282–2288.
[30] F. Zhou, K. Adachi, K. Kato, Sliding friction and wear property of a-C and a-CN_x coatings against SiC ball in water, Thin Solid Films 514 (2006) 231–239.